RSC Advances

ROYAL SOCIETY OF CHEMISTRY

www.rsc.org/advances

Preparation of a silica nanospheres/graphene oxide hybrid and its application in phenolic foams with improved mechanical strengths, friability and flame retardancy

Xiaoyan Li[a], Zhengzhou Wang[a,b*], Lixin Wu[c,]

[a] School of Materials Science and Engineering, Tongji University, Shanghai 201804, P.R. China;

[b] Key Laboratory of Advanced Civil Engineering Materials (Tongji University), Ministry of Education, Shanghai 201804, P.R. China

[c] State Key Laboratory of Structural Chemistry, Fujian Institute of Research on the Structure of Materials, Chinese Academy of Sciences, Fuzhou 350002, China

Abstract

A silica nanospheres/graphene oxide hybrid (SGO) was successfully synthesized through immobilization of silica (SiO_2) nanospheres on the surface of graphene oxide (GO) sheets, and characterized by X-ray diffraction (XRD), field emission scan electronic microscopy (FESEM) and transmission electronic microscopy (TEM). It has been found that the incorporation of the SGO into the phenolic (PF) foams not only obviously increases the mechanical strengths and flame retardancy, but also reduces the pulverization ratio. Specifically, the flexural and compressive strengths of the PF foam modified by 1.5 phr SGO increases by 31.6 % and by 36.2 %, respectively, compared with pure PF foam. The Cone calorimetric results indicate that the addition of SGO into PF foam leads to a reduction in peak heat release rate and total heat release. Moreover, the thermal stability of the PF foams containing SGO is enhanced compared with the pure PF foam.

Keywords: Mechanical strengths, Flame retardancy, Phenolic foams, Silica nanospheres/graphene oxide hybrid

1. Introduction

Polymeric foams, such as polystyrene (PS) and polyurethane (PU) foams, are widely used in the fields of construction.[1, 2] Unfortunately, the poor flame retardancy of PS and PU foams usually

* Correspondence to Z Wang, Email: zwang@tongji.edu.cn, Fax:0086-21-69590076

lead to fires generating abundant smoke and toxic gases, which are harmful to people on the spot.[3] In comparison, phenolic (PF) foams have many advantages, for example, excellent fire resistance, no dripping and low production of toxic gases during combustion, high thermal stability, good thermal insulation,[4-6] *etc*. However, the brittleness and pulverization of PF foams severely restrict their applications.[7] Therefore, it is very significant to improve the toughness of the foams, meanwhile, maintaining their excellent flame resistance.

In general, the toughness of PF foams can be improved by two types of additives: organic polymers and micro or nano-scale fillers. The polymeric toughening agents used for PF foams include polyvinyl alcohol (PVA),[8] polyethylene glycol (PEG),[9] nitrile butadiene rubber powder,[10] epoxy resin,[11] *etc*. However, the excellent fire-retardant performance of PF foams deteriorates due to the introduction of these combustible polymeric toughening agents. In order to overcome this problem, several flame retardant toughening agents, such as phosphorus-containing polyurethane[12] and phosphorus-containing polyethers,[13] were synthesized to improve the toughness and flame retardancy of PF foams at the same time. Another way to solve the problem of PF foams is the introduction of micro or nano-scale fillers, such as fibers, clays, carbon nanotubes (CNTs) and graphene. For example, Zhou *et al.* incorporated glass fiber as a reinforced agent into PF foams, and found that the mechanical properties of PF foams were improved, and the reinforced foams have a smaller thermal expansion coefficient and higher storage modulus compared with unreinforced foam.[14] Hu *et al.* developed glass fiber/nanoclay reinforced PF foam, and confirmed that glass fiber and nanoclay demonstrated good synergistic effects in increasing the toughness, flame retardancy and compressive strength of PF foams.[15] Niu *et al.* infused the organo-modified montmorillonite in the synthesis step of cardanol PF resin to produce nanocomposite PF foams, and these platelets can be exfoliated and dispersed well in the nanocomposite, and improve the thermal stability, fire resistance and mechanical properties of the nanocomposite foams.[16] Yang *et al.* reinforced PF foams with functionalized multiwalled carbon nanotubes (MWCNTs) and found that carboxyl multi-walled carbon nanotubes could increase the compressive strength and thermal stability, while maitain the excellent flame retardancy of the foams.[17]

Graphene due to its unique layered and graphitized sheet structure has been applied into polymeric foams to improve their mechanical properties and thermal properties. For example, Yan

et al. introduced graphene nanosheets (GNSs) and carbon nanotubes (CNTs) into rigid polyurethane foam (RPUF), and found that GNSs worked more effectively than CNTs in mechanical property and heat resistance enhancement of the RPUF foam.[18] Yang *et al.* prepared polystyrene/graphene nanocomposite foams using supercritical carbon dioxide, and their results showed that the well exfoliated GO sheets could be a high efficient nucleation agent to improve thermal stability and dynamic mechanical properties.[19] Recently, Zhou *et al.* found that friability and mechanical properties of PF foam reinforced with GO sheets had been improved greatly because of powerful interfacial adhesion between GO sheets and PF foam matrix.[20]

However, graphene tends to decompose during combustion due to its weak thermal-oxidative stability, which destroys its unique layered structure affecting its flame retardant effect.[21] Therefore, it is very significant to increase flame retardant efficiency of graphene by surface modification.[22-24] Herein, a novel silica nanospheres/graphene oxide hybrid (SGO) was prepared through immobilization of SiO_2 nanospheres on the surface of GO sheets. Then SGO was incorporated into PF foams to study its effect on the mechanical strengths, thermal stability, pulverization ratio and flame retardancy.

2. Experimental

2.1. Materials

Natural graphite powder (99.95% metals basis, 750-850 mesh), 1,3,5-trimethylbenzene (TMB), tetraethylorthosilicate (TEOS) and dimethoxydimethylsilane (DMDMS) were supplied by Aladdin Industrial Co. Ltd (China). Pluronic F108 ($EO_{132}PO_{50}EO_{132}$, where EO is polyethylene oxide and PO is polypropylene oxide) were obtained from Sigma-Aldrich company. H_2SO_4 (98%), hydrochloric acid, $NaNO_3$, $KMnO_4$, hydrogen peroxide (30%), Tween 80, p-toluenesulfonic acid, n-pentane, phosphoric acid and ethanol were all commercial products with analytical grades purchased from Sinopharm Chemical Reagent Co. (Shanghai, China), and used without further purification. Resol type PF resin was supplied by Shandong Shengquan Chemical Co., Ltd. (Shandong, China).

2.2. Preparation of graphene oxide

Graphene oxide (GO) was prepared and purified by Hummers method.[25] Typically, 2.0 g graphite, 2.0 g $NaNO_3$ and 80 mL of 98 wt% H_2SO_4 were added to a three-necked bottle with vigorous stirring for 2 h in an ice bath. Subsequently, 10 g $KMnO_4$ was slowly added, and the mixture was reacted at 35 ^oC for 2 h. Then 200 mL of 5 % dilute sulfuric acid was slowly added to the mixture which was stirred for 2 h at 60 ^oC. The temperature was raised to 95 ^oC and the aqueous solution of hydrogen peroxide (30 %, 20 ml) and distilled water (1000 ml) were added slowly. The mixture was stirred for 1 h at 95 ^oC. Finally, a brown solid was collected by centrifugal and washed with hydrochloric acid until the manganese and sulfate ions were completely removed. The brown solid was dried at 60 ^oC for 24 h in a vacuum oven before being used.

2.3. Preparation of silica nanospheres/graphene oxide hybrid

SiO_2 nanospheres and SiO_2 nanospheres/GO hybrid (SGO) were prepared by previous reported method.[26, 27] Typically, 1.0 g pluronic F108 and 1.0 g 1,3,5-trimethylbenzene (TMB) were mixed into 30 mL HCl solution (2.0 M), and the mixture was kept stirring for 6 h at 25 °C. Then, 1.0 g TEOS was added dropwise into the suspension under vigorous stirring. After reacting for 6 h, 0.5 g Dime thoxydimethylsilane (DMDMS) was introduced into the system and the reaction was continued for another 48 h. The resulted mixture was dialyzed for 48 h and it was diluted to 60 mL by distilled water to obtain the aqueous solution of SiO_2 nanospheres. GO suspension (600 mL, 1.0 mg/mL^{-1}) was mixed with 60 ml aqueous solution of SiO_2 nanospheres and the whole system was left to stir for 12 h at room temperature. Then, the solid precipitate was collected by centrifugation at 4000 rpm and washed with ethanol. The SGO hybrid was obtained after drying in an oven at 60 °C.

2.4. Preparation of toughened PF foams

Phenolic resin (5 g), GO, SiO_2 nanospheres and SGO were mixed in a certain ratio, and then curing agent (6 phr, p-toluenesulfonic acid/phosphorous acid/distilled water = 1:2:2 by weight), surfactant (Tween 80, 3 phr), and blowing agent (n-pentane, 4 phr) were mixed at room temperature under rapid stirring and treated by ultrasonic. And then the mixture was poured into a mold. After curing for 60 min at 80 °C, the toughened PF foams were obtained. The formulations

are given in Table 1. To keep the density of the foams identical (16 ± 0.5 kg/m^3), the same amount of the mixture was put into the mold. The foams were carefully cut for properties testing.

2.5. Characterization and measurements

Surface morphologies were observed through field emission scan electronic microscopy (FESEM, Hitachi S-4800) and transmission electronic microscopy (TEM, JEOL JEM2011). The microstructure of foams was observed by using a XPL-30TF transflective polarizing microscope (Shanghai Weitu Instrument Co., Shanghai, China) on transmission types. X-ray diffractions (XRD) were performed on a Rigaku D/maxr B diffractometer with Cu Ka radiation.

The flexural strength of the foams was measured by a CMT5105 universal testing machine, according to GB/T 20974-2014 (specified GB/T8812.1-2007). Each specimen used for the test was 120 × 25 × 20 mm^3. The compressive strength of the foams was measured by a DXLL-5000 universal testing machine according to GB/T 20974-2014 (specified GB/T8813-2008). Each specimen used for the test was 50 × 50 ×50 mm^3. In both measurements, at least five samples were tested to obtain average values. The density was determined according to the dimensions and the weight of the foam.

Thermogravimetric analysis (TGA) tests were carried out by using a STD Q600 (simultaneous differential scanning calorimetry−TGA) thermo-analyzer instrument (TA Co., New Castle, DE, USA) at a heating rate of 10 °C/min under nitrogen flow. The weight of all samples was kept within 5 mg in an Al_2O_3 pan, and samples were heated from room temperature to 800 °C

Cone calorimetric tests (CCT) were carried out on a FTT cone calorimeter (dual) according to the standards of ISO 5660. Each specimen used for the test was 100 × 100 × 20 mm^3. The heat flux for testing was 35 kW/m^2.

The limiting oxygen index (LOI) was measured by an HC-2 oxygen index meter, according to GB/T2406-2009. Each specimen used for the test was 100 × 10 × 10 mm^3.

The UL 94 vertical test was carried out on a CFZ-3-type horizontal and vertical burning tester according to GB/T2408-2008. Each specimen used for the test was 130 × 13 × 3 mm^3.

Pulverization ratio was measured by the weight loss of foams after friction. Each specimen used for testing was 20 × 20 × 20 mm^3. Those samples were first loaded with a 50 g weight and then pushed back and forth with a constant force 30 times on fixed sandpaper. Each single-pass

friction distance was 250 mm. Pulverization ratios were calculated according to Equation 1:

$$\text{Pulverization ratio} = (M_1-M_2)/M_1\times 100\% \quad (1)$$

where M_1 is the weight before friction and M_2 is the weight after friction.

3. Results and discussion

3.1. Characterization of GO, SiO_2 nanospheres and SGO

Figure 1 presents the XRD patterns of GO, SiO_2 nanospheres and SGO. Compared with the peak of natural graphite at $2\theta = 24.4^o$, the GO peak appear at $2\theta = 12.1°$corresponds to a d-spacing of 0.726 nm resulting from the insertion of hydroxyl, carboxyl and epoxy groups between the graphite sheets as a result of the oxidation process of natural graphite.[28] The XRD pattern of SiO_2 nanospheres shows an abroad peak centered at $2\theta =22.9^o$ which corresponds to d-spacing of 0.387 nm，and it is attributed to the peak of the SiO_2 nanospheres.[29] In the case of the pattern of SGO, after the immobilization process of SiO_2 nanospheres on the GO sheets, the GO peak shifts from $2\theta = 12.1°$ to $2\theta = 8.61^o$ which correspond to d-spacing of 1.03 nm, and the amorphous peak around at $2\theta =22.9^o$ results from SiO_2 nanospheres. This suggests the successful immobilization of SiO_2 nanospheres on the surface of GO sheets during the immobilization process.[27]

The structure and morphology of GO, SiO_2 nanospheres and SGO were also investigated by field emission scan electronic microscopy (FESEM) and transmission electron microscopy (TEM). As shown in Figure 2, it can be clearly seen that the GO structure exhibits a sheet-like multilayer morphology and the GO sheets stack together under the SEM observation. The TEM image of GO (Figure 2d) also shows the sheet-like structure with some drapes. From the FESEM and TEM images (Figure 2b and 2e), it can be found that the SiO_2 nanospheres are hollow, and possess a uniform particle size of around 20.0 nm，a cavity diameter of ca. 11.5 nm, and a wall thickness of ca. 6.5nm.[26] After the self-assembly of between GO sheets and SiO_2 nanospheres, the SiO_2 nanospheres are successfully immobilized on the surface of GO sheets. FESEM and TEM observations of the SGO (Figure 2c and 2f) exhibit a sheet-like morphology composed of multilayered nanostructures, and the SiO_2 nanospheres are embedded into the interlayer of GO sheets and tightly adhere to the surface, demonstrating a specific affinity between the hydrophobic SiO_2 nanospheres and GO sheets.

3.2. Microstructures of toughened PF foams

To study the effect of the nanofillers on the microstructures of PF foams, foam samples were observed with an optical microscope. As shown in Figure 3, it can be clearly seen that the structure of the foams are mainly closed cells. Meanwhile, the cell sizes of sample 0.5SGO/PF is slightly smaller than the ones of sample 0.5GO/PF (Figure 3b), 0.5SiO_2/PF (Figure 3c) and pure PF (Figure 3a), and the cell structure of sample 0.5SGO/PF is also more uniform. This result is probably attributed to the differences of the dispersion and surface character between the polymer and these three nanofillers during the process of heterogeneous nucleation in polymer foams. Compare with GO, the surface of SGO due to the immobilization of SiO_2 nanospheres changes from hydrophilic to hydrophobic, which favours the effectiveness of the nucleation of SGO in the PF foams.[30] In addition, the easy agglomeration of SiO_2 nanospheres also makes it difficult to uniformly disperse in the PF matrix, which is adverse to the process of heterogeneous nucleation. Therefore, the cell structure of sample 0.5SGO/PF is better than that of samples 0.5GO/PF and 0.5SiO_2/PF.

Besides, compared with pure PF foam, the cell sizes for SGO-toughened PF foams show a decreasing tendency with the increase of dosage of SGO. Such tendency can be explained by the reason that the nanofiller SGO as a nucleating agent during the foaming process generated more cells, and thus cell sizes of its toughened PF foams are smaller than that of pure PF foam, which result in an increase in the cell density relatively.[31] However, the distribution of cell sizes of sample 2.0SGO/PF is not very uniform, and the reason for it is due to easy agglomeration of SGO at a higher loading (2.0 phr).[32]

3.3. Properties of toughened PF foams

3.3.1. Mechanical properties

Figure 4 shows flexural and compressive strengths of pure and toughened PF foams by the nanofillers. The flexural and compressive strengths of the toughened foams are improved compared with those of the pure PF foam. This result can be explained by two reasons: first of all, the added nanofillers are inserted into the cell walls of the foams and increase the strengths of the

cell walls because of the high strength of nanofillers; secondly, the nanofillers, which function as a nucleating agent, are introduced into the PF foams to increase the cell density and generate more small cells，resulting in higher compressive strength of PF foams because they have more cell ribs and cell walls that undergo external force.[15] As shown in Figure 4, the flexural and compressive strengths of SGO-toughened PF foam are slightly higher than those of the GO and SiO_2-toughened PF foams. On one hand, the origin of SGO sheets reinforcement may be caused by its ultrahigh aspect ratio and good interaction with PF resin matrix, which provide additional constraints to the segmental movement of the polymer chains of PF foams.[18] The good interaction with PF resin matrix can be attributed to the formation of ester bonds between carbonyl (–COOH) groups on SGO and hydroxyl (–OH) groups on PF resin at high temperatures in the acidic condition, which is beneficial to the improvement of mechanical strengths.[20] On the other hand, the modification of hydrophobic SiO_2 nanospheres on the surface of GO sheets benefits heterogeneous nucleation of nanofiller SGO in PF foams, resulting in generating more cells to resist external force and improve the mechanical properties. Based above reasons, SGO-toughened PF foam shows higher mechanical strengths than those of the GO and SiO_2-toughened PF foams.

As shown in Figure 5, with increasing content of SGO, the flexural and compressive strengths of the toughened PF foams first increase, reach the maximum values at 1.5 phr SGO, and after that loading decrease slightly. Compared with pure PF foam, the flexural and compressive strengths of SGO-toughened PF foam at 1.5 phr SGO increases by 31.6 % (from 0.136 to 0.179 MPa) and by 36.2 % (from 0.058 to 0.079 MPa), respectively. The highest strengths are due to uniform cell morphology and smaller cell size, which can undergo high external force. The decrease in flexural and compressive strengths of sample 2.0SGO/PF at a higher loading (2 phr) may be caused by the agglomeration of SGO particles and their poor dispersion in the PF resin. The above results indicate that an appropriate addition of SGO is helpful to improve the mechanical strengths of PF foams.

3.3.2. Pulverization ratios

The high friability of PF foams tends to cause a severe problem. Hence, it is essential to overcome the problem of PF foams in order to expand their applications. The pulverization ratios

of pure and toughened PF foams are shown in Figure 6. Compared with the pure PF foam, the pulverization ratios of the PF foams toughened by the nanofillers are all improved. Moreover, it is clear that the pulverization ratio first decreases gradually with an increase in the content of SGO, and then increases slightly at 2 phr loading. This can be attributed to ultrahigh aspect ratio, good interaction of SGO with PF resin and promotion of heterogeneous nucleation, thus further reducing the pulverization ratio. The slight increase in the pulverization ratio for sample 2.0SGO/PF may be caused by the defect of cell structure resulting from the appearance of agglomeration problem of SGO at a higher loading.

3.3.3. Flame retardant properties

LOI and UL 94 rating

To evaluate the flame retardant effect of nanofillers, pure and toughened PF foams were measured by the limiting oxygen index (LOI) and UL 94 vertical burning tests. The results are presented in Table 2. It can be seen from Table 2 that the LOI of the SGO-toughened PF foam is higher than that of GO and SiO_2-toughened PF foams, indicating some synergistic effect in flame retardancy between GO and SiO_2 nanospheres. The LOI of the SGO-toughened PF foams increases gradually with increasing the SGO content. At 0.5, 1.5 and 2.0 phr loadings of SGO, the LOI values are 39.5 %, 40.5 % and 41.0 %, respectively. The increase in LOI is probably because the SiO_2 nanopspheres covered on the surface of GO sheets can hinder the decomposition of GO sheets, and thus maintain the physical barrier effect of the sheets to the heat and mass transfers at high temperatures.[33] Moreover, the higher cell density caused by the SGO helps to increase the flame resistance of foam. Besides, all the foams can pass the UL 94 V0 rating.

Cone calorimetric tests

Figure 7 shows the curves of heat-release rate (HRR) from cone calorimetric analyses of pure and toughened PF foams, and the typical data are also summarized in Table 3. The peak heat-release rate (PHRR), the mean heat-release rate (mHRR) and the total heat release (THR) of toughened PF foams are all lower than those of pure PF foam. Specially, compared with pure PF foam, sample 1.5SGO/PF displays 21.4 % and 6.4 % reduction in the PHRR and THR,

respectively, while their values of time to ignition also increases 10 s. Compared with GO-toughened PF foam, SGO-toughened PF foam has lower mHRR and THR values. The increase in the loading of SGO leads to a further decrease in PHRR, mHRR and THR values.

3. 4. Thermal decomposition of toughened PF foams

TGA and derivative thermogravimetric (DTG) measurements were used to investigate the thermal decomposition of pure and toughened PF foams. The results are shown in Figure 8 and Figure 9, and some decomposition data are listed in Table 4. It can be seen from the DTG curves (Figure 9) that pure PF foam has four stages of decomposition. The first one, occurring below 100 °C, is mainly caused by to the volatilization of residual moisture and blowing agents in the foam. The second decomposition step at about 160 °C may be on account of the dehydration of further curing of PF foams.[34] The third stage happens in a temperature range, from 250 °C to nearly 400 °C, and the weight loss may be attributed to the degradation of surfactants (i.e. Tween 80). The fourth stage from 400 to 800 °C is due to the decomposition of cured PF resin in the foam with a T_{max} (the peak temperature in the DTG curve) of 467.8 °C. The toughened PF foams by the nanofillers also show four similar decomposition stages. Compared to the pure PF foam, the toughened foams show higher thermal stability, and their $T_{-5\%}$ (the temperatures at 5 % weight loss), $T_{-30\%}$ (the temperatures at 30 % weight loss) and T_{max} of GO, SiO_2 and SGO-toughened PF foams all increase as shown in Table 4. The values and residues at 750 °C of SGO-toughened PF foam are all higher than those of SiO_2 and GO-toughened PF foam at the same loading, the reason is probably that the SiO_2 nanopspheres immobilized on the surface of GO sheets can hinder the decomposition of GO sheets, and thus enhance the thermal stability of the PF foams.

4. Conclusions

A graphene-based hybrid (SGO) consisting of GO sheets and SiO_2 nanospheres was prepared through immobilization of SiO_2 nanospheres on the surface of GO sheets. FESEM and TEM images confirm that the hollow SiO_2 nanospheres with a particle size of around 20.0 nm are uniformly deposited on the surface of GO sheets. The incorporation of 1.5 phr SGO into PF foam

leads to a 31.6% increase in the flexural, a 36.2% increase in compressive strength, and an about 70% decrease in the pulverization ratio. The Cone calorimetric results indicate that the SGO modified PF foam has a lower peak heat release rate and total heat release than the pure PF foam. Moreover, the thermal stability of the PF foams containing SGO is enhanced compared with the pure PF foam.

Acknowledgements

This work was financially supported by the National Natural Science Foundation of China (Nos. U1205114/L11 and 21174106).

References

1. M. M. Bernal, M. Martin Gallego, I. Molenberg, I. Huynen, M. A. Lopez Manchado and R. Verdejo, *RSC Adv.*, 2014, **4**, 7911.
2. H. Zhang, Y. Y. Kuo, A. C. Gerecke and J. Wang, *Environ. Sci. Technol.*, 2012, **46**, 10990.
3. A. A. Stec and T. R. Hull, *Energy and Buildings*, 2011, **43**, 498.
4. C. J. Tseng and K. T. Kuo, *J. Chin. Inst. Eng.*, 2002, **25**, 753.
5. S. Lei, Q. Guo, J. Shi and L. Liu, *Carbon*, 2010, **48**, 2644.
6. H. Shen, A. J. Lavoie and S. R. Nutt, *Composites Part A: Applied Science and Manufacturing*, 2003, **34**, 941.
7. L. Pilato, *Reactive and Functional Polymers*, 2013, **73**, 270.
8. T. Horikawa, K. Ogawa, K. Mizuno, J. I. Hayashi and K. Muroyama, *Carbon*, 2003, **41**, 465.
9. M. Gao, Y. L. Yang and Z. Q. Xu, *Advanced Materials Research*, 2013, **803**, 21.
10. L. Li, Y. Z. Xu, C. P. Wang and F. X. Chu, *Applied Mechanics and Materials, Trans Tech Publ,* 2012, **204**, 4137.
11. M. L. Auad, L. Zhao, H. Shen, S. R. Nutt and U. Sorathia, *Journal of Applied Polymer Science*, 2007, **104**, 1399.
12. H. Yuan, W. Xing, H. Yang, L. Song, Y. Hu and G. H. Yeoh, *Polymer International*, 2013, **62**, 273.
13. H. Yang, X. Wang, H. Yuan, L. Song, Y. Hu and R. K. Yuen, *Journal of Polymer Research*, 2012, **19**, 1.
14. J. Zhou, Z. Yao, Y. Chen, D. Wei and Y. Wu, *Materials & Design*, 2013, **51**, 131.
15. X. Hu, W. Cheng, W. Nie and D. Wang, *Polymer Composites*, 2015 (DOI: 10.1002/ pc.23411).
16. M. Niu and G. J. Wang, *Advanced Materials Research, Trans Tech Publ,* 2013, **712**, 147.
17. Z. Yang, L. Yuan, Y. Gu, M. Li, Z. Sun and Z. Zhang, *Journal of Applied Polymer Science*, 2013, **130**, 1479.
18. D. Yan, L. Xu, C. Chen, J. Tang, X. Ji and Z. Li, *Polymer International*, 2012, **61**, 1107.
19. J. Yang, L. Huang, L. Li, Y. Zhang, F. Chen and M. Zhong, *Journal of Polymer Research*, 2013, **20**, 1.

20. J. Zhou, Z. Yao, Y. Chen, D. Wei and T. Xu, *Polymer Composites*, 2014, **35**, 581.
21. P. Liu, Y. Huang and X. Zhang, *Composites Science and Technology*, 2014, **95**, 107-113.
22. C. Bao, L. Song, C. A. Wilkie, B. Yuan, Y. Guo, Y. Hu and X. Gong, *Journal of Materials Chemistry*, 2012, **22**, 16399.
23. X. Wang, L. Song, H. Yang, W. Xing, B. Kandola and Y. Hu, *Journal of Materials Chemistry*, 2012, **22**, 22037.
24. X. Wang, S. Zhou, W. Xing, B. Yu, X. Feng, L. Song and Y. Hu, *Journal of Materials Chemistry A*, 2013, **1**, 4383.
25. W. S. Hummers Jr and R. E. Offeman, *Journal of the American Chemical Society*, 1958, **80**, 1339.
26. J. Zhu, J. Tang, L. Zhao, X. Zhou, Y. Wang and C. Yu, *Small*, 2010, **6**, 276.
27. X. Huang, K. Qian, J. Yang, J. Zhang, L. Li, C. Yu and D. Zhao, *Advanced Materials*, 2012, **24**, 4419.
28. H. K. Jeong, Y. P. Lee, R. J. Lahaye, M. H. Park, K. H. An, I. J. Kim, C. W. Yang, C. Y. Park, R. S. Ruoff and Y. H. Lee, *Journal of the American Chemical Society*, 2008, **130**, 1362.
29. L. Gong, H. Zou, G. Wang, Y. Sun, Q. Huo, X. Xu and Y. Sheng, *Optical Materials*, 2014, **37**, 583.
30. M. M. Bernal, S. Pardo Alonso, E. Solórzano, M. Á. Lopez Manchado, R. Verdejo and M. Á. Rodriguez Perez, *Rsc Advances*, 2014, **4**, 20761.
31. C. Yang, Z. H. Zhuang and Z. G. Yang, *Journal of Applied Polymer Science*, 2014, **131**, 1097.
32. S. A. Song, Y. S. Chung and S. S. Kim, *Composites Science and Technology*, 2014, **103**, 85.
33. R. Wang, D. Zhuo, Z. Weng, L. Wu, X. Cheng, Y. Zhou, J. Wang and B. Xuan, *Journal of Materials Chemistry A*, 2015, **3**, 9826.
34. H. Yang, X. Wang, B. Yu, H. Yuan, L. Song, Y. Hu, R. K. Yuen and G. H. Yeoh, *Journal of Applied Polymer Science*, 2013, **128**, 2720.

Legends of Tables

Legends of Figures

Table 1. Formulations of pure and toughened PF foams

Sample code	Phenolic resin (phr)	GO (phr)	SiO_2 nanospheres (phr)	SGO (phr)
Pure PF	100		-	-
0.5SiO_2/PF	100	-	0.5	-
0.5GO/PF	100	0.5	-	-
0.5SGO/PF	100	-	-	0.5
1.0SGO/PF	100	-	-	1.0
1.5SGO/PF	100	-	-	1.5
2.0SGO/PF	100	-	-	2.0

Curing agent (12 phr), Blowing agent (8 phr), Tween 80 (5 phr)

Table 2. LOI and UL 94 rating of pure and toughened PF foams

Sample code	LOI (%)	UL-94 rating
Pure PF	38.0	V0
0.5SiO_2/PF	38.5	V0
0.5GO/PF	38.5	V0
0.5SGO/PF	39.5	V0
1.0SGO/PF	39.5	V0
1.5SGO/PF	40.5	V0
2.0SGO/PF	41.0	V0

Table 3. Cone calorimetric data of pure and toughened PF foams (35 kW/m^2)

Sample code	TTI [a] (s)	PHRR [b] (kW/m^2)	mHRR [c] (kW/m^2)	THR [d] (MJ/m^2)
Pure PF	17	27.6	16.9	3.1
0.5SiO_2/PF	22	20.3	11.4	2.1
0.5GO/PF	23	26.0	19.3	3.5
0.5SGO/PF	27	26.1	17.4	3.1
1.5SGO/PF	27	21.7	16.5	2.9

[a]Time to ignition. [b]Peak heat release rate. [c]Mean heat release rate. [d]Total heat release.

Table 4. TGA and DTG data of pure and toughened PF foams

Sample code	$T_{-5\%}$ (°C)	$T_{-30\%}$ (°C)	T_{max} (°C)	Residue at 750 °C (%)
Pure PF	162.5	452.8	467.8	45.1
0.5SiO_2/PF	176.5	462.1	469.6	47.4
0.5GO/PF	171.9	457.3	469.0	46.5
0.5SGO/PF	172.2	460.0	470.0	47.5
1.0SGO/PF	190.2	463.5	468.5	46.8
1.5SGO/PF	192.1	465.2	470.2	47.6
2.0SGO/PF	199.1	472.1	472.1	48.9

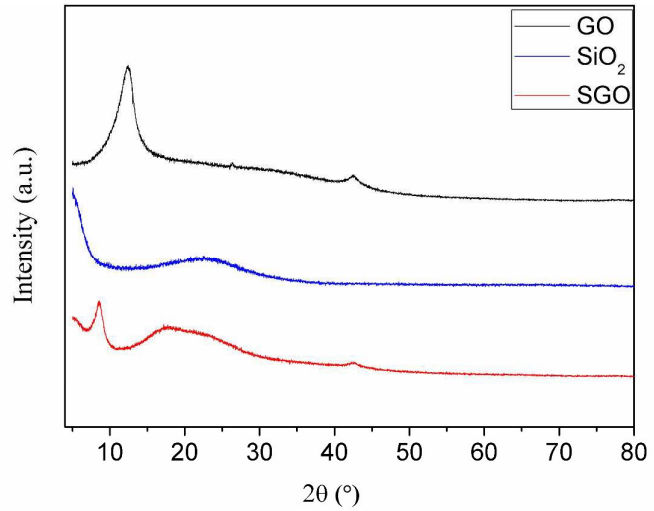

Figure 1. XRD patterns of GO, SiO_2 nanospheres and SGO

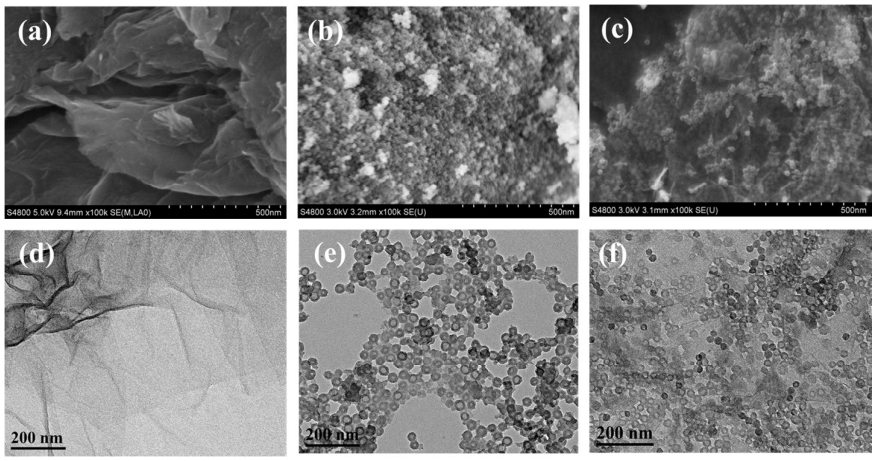

Figure 2. SEM images of (a) GO, (b) SiO_2 nanospheres, and (c) SGO; TEM images of (d) GO, (e) SiO_2 nanospheres, and (f) SGO

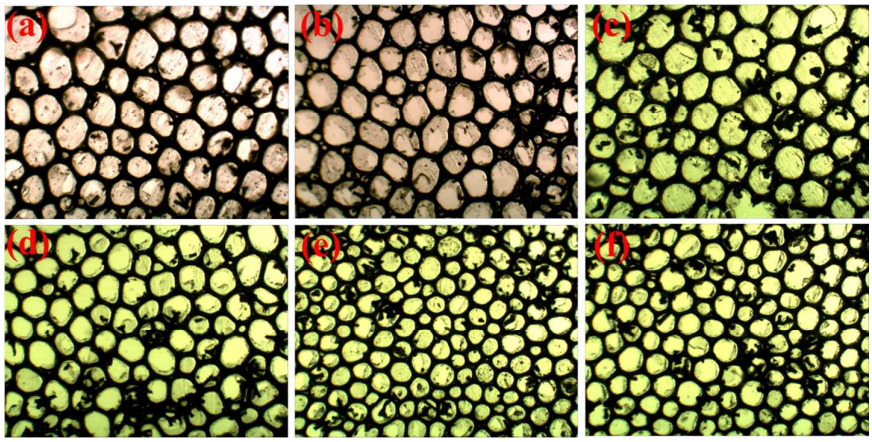

Figure 3. Optical images of (a) pure PF foam and PF foams toughened by (b) 0.5GO/PF, (c) 0.5SiO_2/PF, (d) 0.5SGO/PF, (e) 1.5SGO/PF, (f) 2.0SGO/PF. The magnification of all images was 40×

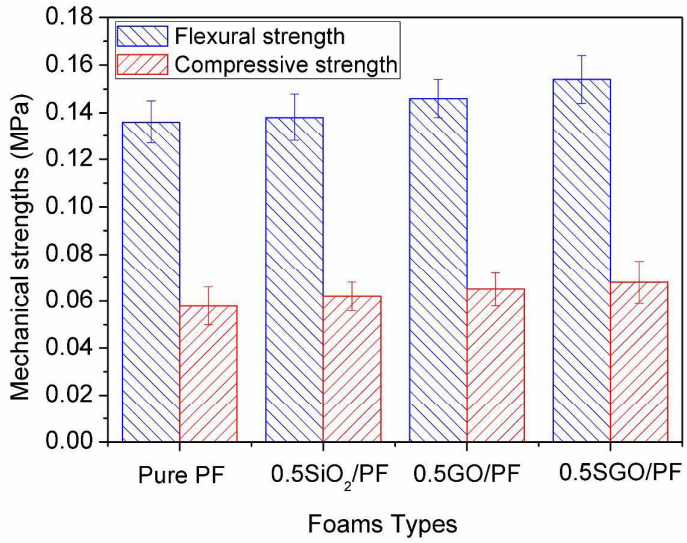

Figure 4. Flexural and compressive strengths of pure and toughened PF foams

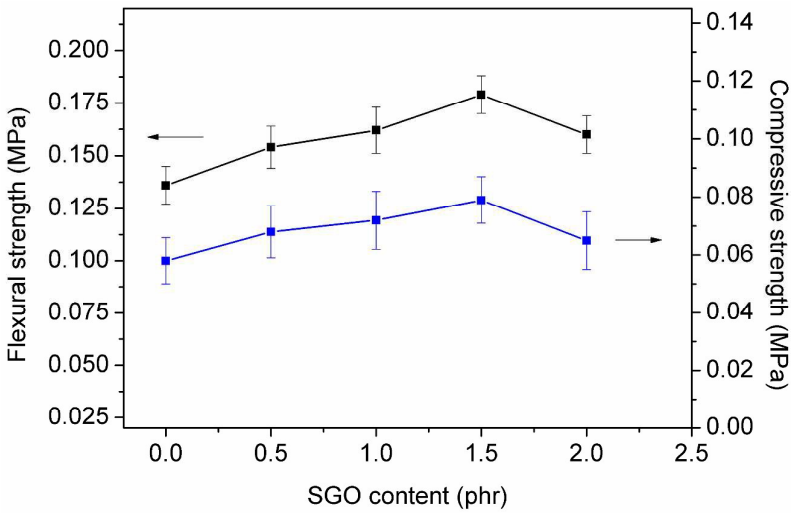

Figure 5. Effect of SGO content on flexural and compressive strengths of PF foams

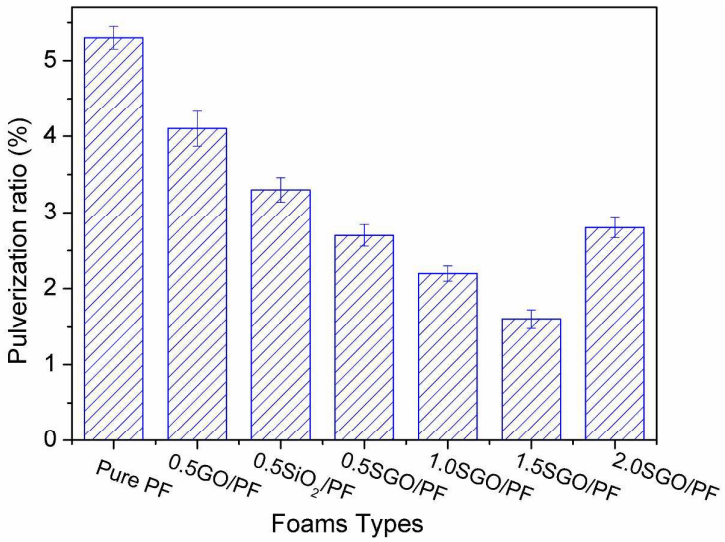

Figure 6. Pulverization ratios of pure and toughened PF foams

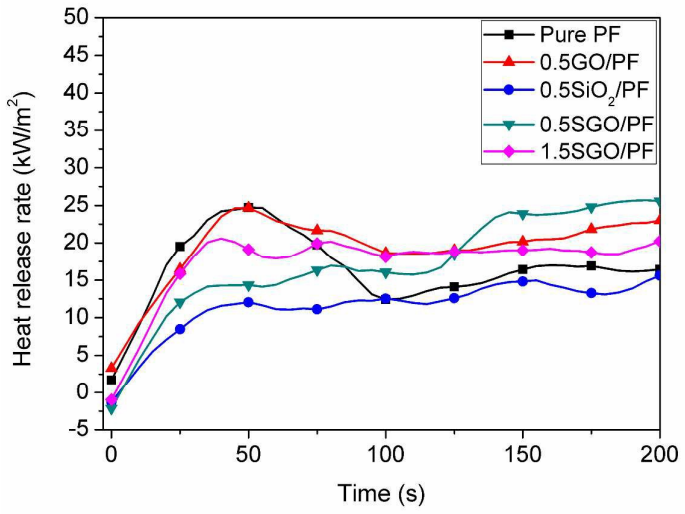

Figure 7. Heat-release rate curves of pure and toughened PF foams (35 kW/m^2)

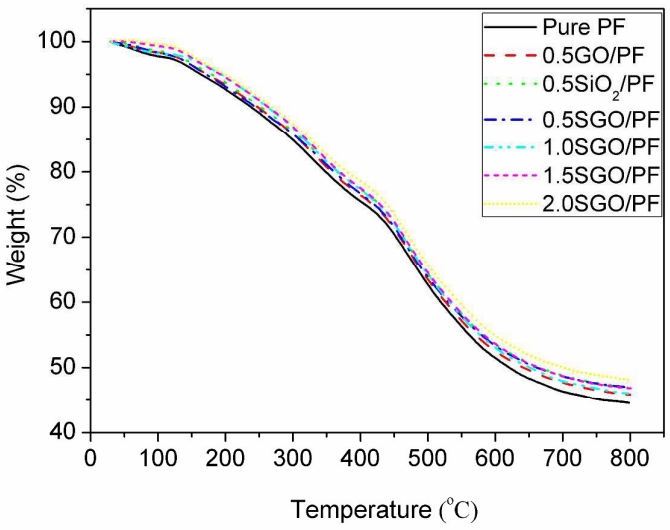

Figure 8. TGA curves of pure and toughened PF foams

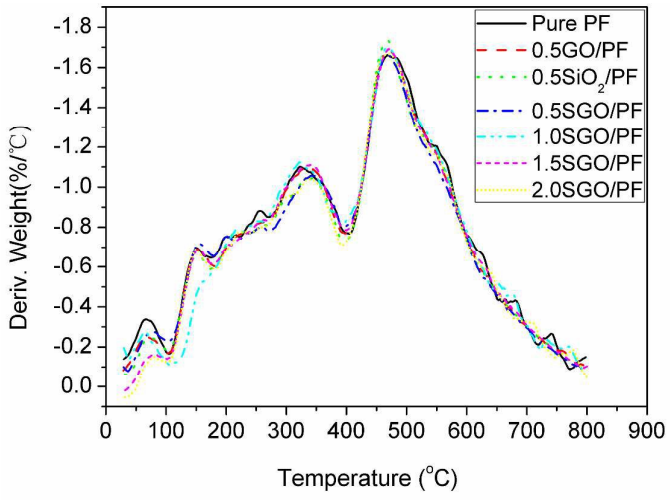

Figure 9. DTG curves of pure and toughened PF foams

Graphic Abstract

A silica nanospheres/graphene oxide hybrid (SGO) was successfully synthesized through immobilization of silica (SiO_2) nanospheres on the surface of graphene oxide (GO) sheets. The incorporation of SGO into phenolic (PF) foam can not only increase the mechanical strengths and thermal stability, but also reduce the pulverization ratio and flammability of PF foams.